Journal of Marine Research, 41, 127-162, 1983

Quasi-Lagrangian structure and variability of the subtropical western North Atlantic circulation

by Stephen C. Riser[1] and H. Thomas Rossby[2]

ABSTRACT

A large body of quasi-Lagrangian trajectory (SOFAR float) data collected from 1976-1979 from 700 m and 2000 m in the western North Atlantic is examined, and it is shown that the character of the trajectories varies markedly over regions as small as a few degrees of latitude and longitude. Kinetic energy increases to the north and west in the basin at both levels. At 700 m a large northwest energy gradient is present between 30N and 31N at 70W. At 2000 m kinetic energy increases to the north and west with the largest gradients very near to the Blake Escarpment at the western boundary of the basin. At both levels the region in the vicinity of 28N, 70W appears to be locally a minimum of kinetic energy. At very low temporal frequencies the trajectories indicate that zonal motions are more energetic than meridional away from the western boundary in the thermocline. At the deeper level the trajectories appear to be influenced by the local bottom topography, though at 2000 m over very flat areas such as the Nares Abyssal Plain zonal motions appear to dominate over meridional at low frequencies as in the thermocline.

From the data it is possible to examine three regions of the subtropical western North Atlantic. North of approximately 32N and west of 60W, there is evidence of a westward recirculation in the thermocline, based on one very long trajectory. To the south of the recirculation regime in the greater MODE region (25-30N, 67-75W) there is evidence that individual fluid parcels in the thermocline undergo large rms displacements but small net displacements from their initial positions over times of the order of a year and may remain in this region for a period of several years. To the south and east of the MODE region there is repeated evidence of the presence of a well-defined eastward flow in the thermocline of approximately 4 cm sec^{-1}, extending zonally at least to the eastern edge of the sampled region.

At 2000 m, a southerly mean flow is present west of 67W and south of 32N, and there is indication that very near to the western boundary in this region the southerly deep transport can be sizeable. In many respects the 2000 m trajectories examined here from west of 67W are both qualitatively and quantitatively similar to the much larger body of trajectory data collected during MODE-I and discussed by Freeland *et al.* (1975). Trajectories from east of 67W at 2000 m show much lower kinetic energy levels than their more western counterparts, and the trajectories of three instruments set in the Nares Abyssal Plain region also indicate the possibility of larger horizontal length scales for the energy containing eddies and weaker horizontal dispersion than in the greater MODE region.

1. School of Oceanography, WB-10, University of Washington, Seattle, Washington, 98195, U.S.A.
2. Graduate School of Oceanography, University of Rhode Island, Kingston, Rhode Island, 02881, U.S.A.

1. Introduction

In the past decade, remarkable progress has been made toward understanding the circulation of the North Atlantic. Since the measurements of Swallow and Crease (Crease, 1962), followed by the Soviet POLYGON and the US MODE experiments, there has been a growing awareness of the complexity of the interaction between the transient part of the ocean circulation (the eddies) and the larger scale spatial and temporal mean circulation.

The joint US-USSR POLYMODE experiment, which began in 1976, attempted to sample a larger portion of the North Atlantic than had earlier experiments. US measurements were made over a region of the North Atlantic west of the Mid-Atlantic Ridge using a variety of techniques, for the purpose of sampling the geographically varying properties of the eddy and mean fields. However, in order to study in addition the detailed properties of the eddy field over a limited region, a Local Dynamics Experiment (LDE) was conducted in the western North Atlantic near 31N, 69W, in the region thought to be on the edge of the Gulf Stream recirculation (Stommel *et al.*, 1978; Worthington, 1976, Ebbesmeyer and Taft, 1979).

A principal component of both the geographical exploration experiments and the smaller scale LDE was quasi-Lagrangian observations of current and temperature obtained from tracking SOFAR floats set at several depths in the North Atlantic. An earlier form of this instrumentation was used successfully in MODE (Freeland *et al.*, 1975 [hereafter FRR]; Rossby *et al.*, 1975; Riser *et al.*, 1978) to study both the dispersive character of the eddy field and the spatial structure of the field on a scale considerably larger than the MODE moored arrays and hydrographic surveys. In this paper, we discusss a number of SOFAR float trajectories and temperature data collected from 1976 to 1979 as part of a series of experiments comprising the geographical exploration component of POLYMODE; in general, the LDE data will be discussed elsewhere. The experiments were initialized in several different regions of the western North Atlantic. However, as these are Lagrangian experiments, instruments set in one area may rapidly move into other areas, and, over times of several years, may sample a large section of ocean.

Most of the trajectories discussed here are in a region south of 31N, north of 15N, and west of the Mid-Atlantic Ridge. This is an area which is heretofore largely unexplored. The bottom topography of the region (Fig. 1) ranges from nearly flat to very rough. The dynamics of this region are not well known, and the mean circulation has not been well determined. Moreover, it has been suggested that the region may play a central role in the poleward heat flux of the combined ocean-atmosphere system (von der Haar and Oort, 1973). The data set analyzed here represents a substantial fraction of all direct observations of currents ever collected from the region. In all but a few cases, the floats are at either 700 m, in the main thermocline, or at 2000 m, in the deeper waters.

The paper will proceed as follows. In the next section, using the data set as a

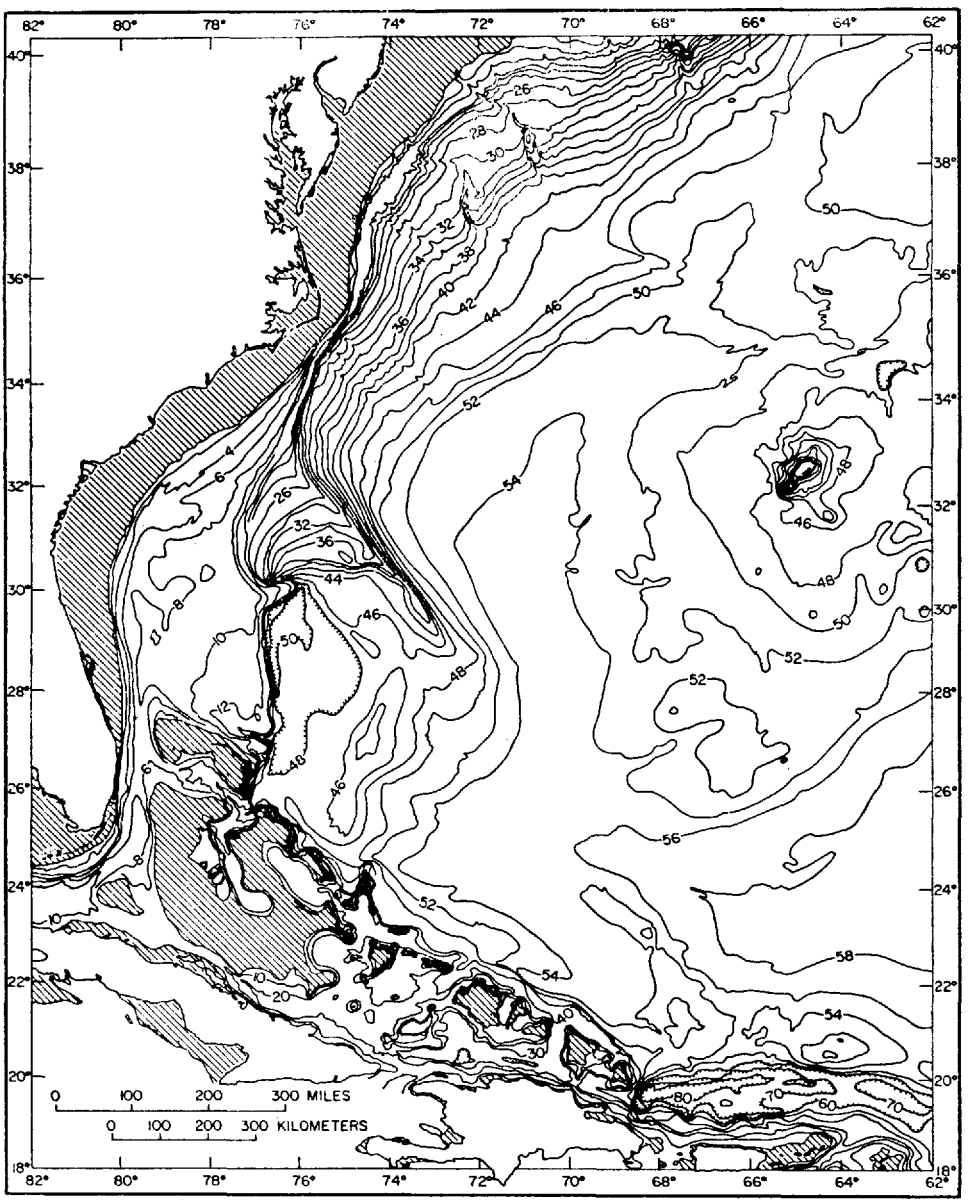

Figure 1. Bottom topography of the western North Atlantic, redrawn from Pratt (1968). Contours are in hundreds of meters.

Table 1. Locations and starting dates of POLYMODE float experiments begun prior to the Local Dynamics Experiment.

Experiment	Number of floats	Starting location	Date
Pre-POLYMODE Test	1	32N, 62W	9/75 (2680)
Nares Abyssal Plain	5	24N, 62W	3/76 (2840)
South Hatteras Abyssal Plain	6	25N, 70W	10/76 (3050)
Western Boundary Region	2	25N, 74W	1/77 (3165)
Hatteras Abyssal Plain	4	26-30N, 70W	4/77 (3245)
Hatteras Abyssal Plain	1	29N, 70W	10/77 (3418)

whole, estimates of the geographical distribution of some properties of the western North Atlantic circulation will be presented, including spatially averaged mean velocities and kinetic energies. In following sections, individual trajectories from experiments in several regions of the western North Atlantic will be analyzed in some detail, and, where possible, the float data will be compared and contrasted to concomitant Eulerian data. Finally, in a Discussion section, we will attempt to interpret the results of our analysis in relation to the existing historical data and contemporary theories of the circulation of the western North Atlantic.

2. Quasi-Lagrangian trajectory data

The trajectory and temperature data to be discussed here represent the results of several distinct experiments. The instrumentation used in these experiments, while in principle similar to that used in MODE (Rossby *et al.*, 1975), was of a new design: floats were actively ballasted to a constant pressure level, and two day running averages of both temperature and pressure along the trajectory were telemetered to the tracking stations as the floats drifted. Details of this instrumentation are given in Webb (1977). Here it is sufficient to note that the telemetered pressures are resolved to approximately 1 decibar, and telemetered temperatures are resolved to .02°C for the 700 m floats and .002°C for the 2000 m floats. In most cases the total tracking errors are less than 5 km. As the floats are ballasted to constant pressure surfaces, they follow only the horizontal projection of particle motion. This implies that a float and a parcel of fluid, coincident in space at some initial instant, will separate with increasing time. Attempts to quantify this apparent diffusion (Riser, 1982a) have shown that, away from the immediate vicinity of intense boundary currents, a float trajectory may often be representative of a fluid parcel trajectory for times of several months.

Locations and dates of the individual experiments are given in Table 1 (time in this paper will be given in modified Julian days, and the relationship of these days to calendar days is given in Table 2). In general, the philosophy behind each of the experiments was one of exploration. The MODE float results (FRR) gave an interesting, though incomplete, picture of the Lagrangian character of the currents

Table 2. Conversion of modified Julian days into calendar days.

Modified Julian day	Calendar day
2500	March 29, 1975
2750	December 4, 1975
3000	August 10, 1976
3250	April 17, 1977
3500	December 23, 1977
3750	August 30, 1978
4000	May 7, 1979

at 1500 m in the southwestern Sargasso Sea. At the beginning of POLYMODE, nearly the entire western North Atlantic, save for the greater MODE region, was largely unexplored either by Lagrangian or Eulerian methods. Thus in an effort to maximize the use of limited resources, it was decided to set small numbers of instruments, typically 4-6, in disparate regions of the western North Atlantic. As the floats were designed to have a lifetime of 2-3 years, it was felt that experiments of this type could provide both some short term information on the dispersive characteristics of the flow fields and also longer term information on the geographically varying properties of the eddy field at two levels in the water column.

a. 700 m data. In Figure 2, the entire data set from 700 m is shown (excluding the data from the LDE). This composite diagram, or spaghetti plot, includes trajectories from 13 different instruments, varying in length from 16 to 829 days.

Even before statistics are computed from this body of data, the eye is seized by several obvious characteristics present in the composite diagram. One feature is the apparent trend for zonal particle displacements to exceed meridional ones away from the immediate vicinity of the western and southwestern boundaries. This appears to be true mainly south of 30N and east of about 70W. Secondly, there is an apparent increase in the spacing between daily fixes, indicating a general increase in speed (and hence, kinetic energy) from southeast to northwest in Figure 2. Thirdly, there is a curious lack of penetration north of about 31N. All of the 13 trajectories presented here began south of 31N, and in the approximately 3 years of data represented on this diagram, only one instrument managed to break away and remain north of 31N.

These qualitative notions may be investigated more quantitatively. Figure 3 is a contour plot of total kinetic energy, computed from the trajectories shown in Figure 2 (in some of the northernmost areas where there is little data, some LDE data are included in these averages as well in order to improve the statistical confidence). These contours have been drawn from total kinetic energies computed by averaging the kinetic energies in 2° by 2° boxes. Estimates of the total kinetic energy for each individual box are also shown in Figure 3.

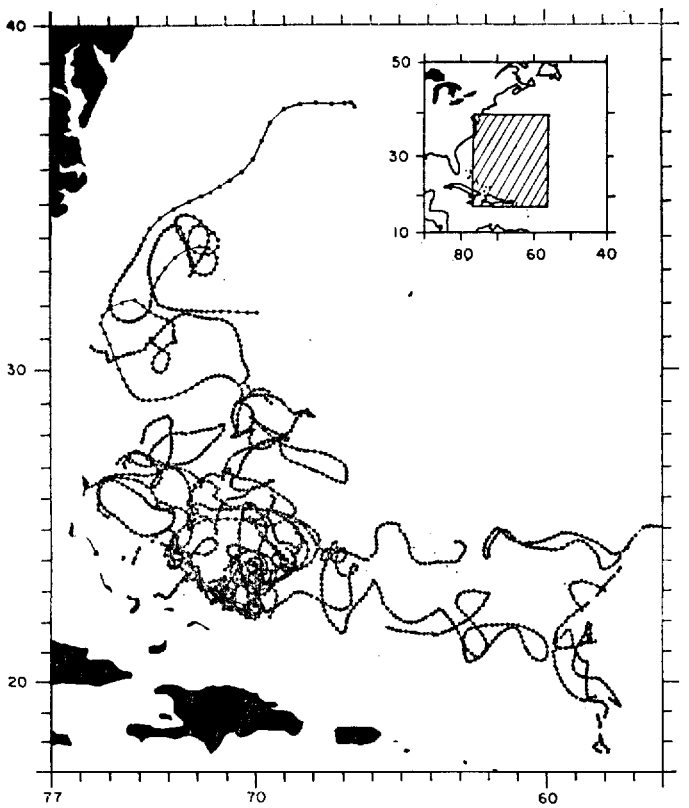

Figure 2. Spaghetti diagram of all 700 m float tracks from 1976 through 1979, excluding data from the POLYMODE Local Dynamics Experiment. Insert shows position in the North Atlantic of this region. One fix per day is plotted on the tracks shown. Short gaps in trajectories have been filled by linear interpolation.

An examination of Figure 3 reveals the anticipated increase in total kinetic energy from southeast to northwest. From 19N to 29N in the western North Atlantic, the energy increases by approximately a factor of two at 700 m; north of 29N, it increases much more rapidly toward the Gulf Stream. Between 29N and 37N, there is roughly an eightfold increase in the level of kinetic energy. While the bulk of the float measurements are considerably farther west than the moored measurements of Schmitz (1978) along 55W, the overall tendency here appears to be very similar to the eight- to tenfold increase in the kinetic energy between 29N and 39N in the thermocline reported in that study.

There is, however, a hint that the kinetic energy distribution at 700 m has a more complicated structure than a simple south to north increase. Kinetic energy also appears to increase to the west, especially between 26-29N. It appears that the region bounded by 29N on the north, 25N on the south, and 73W on the west

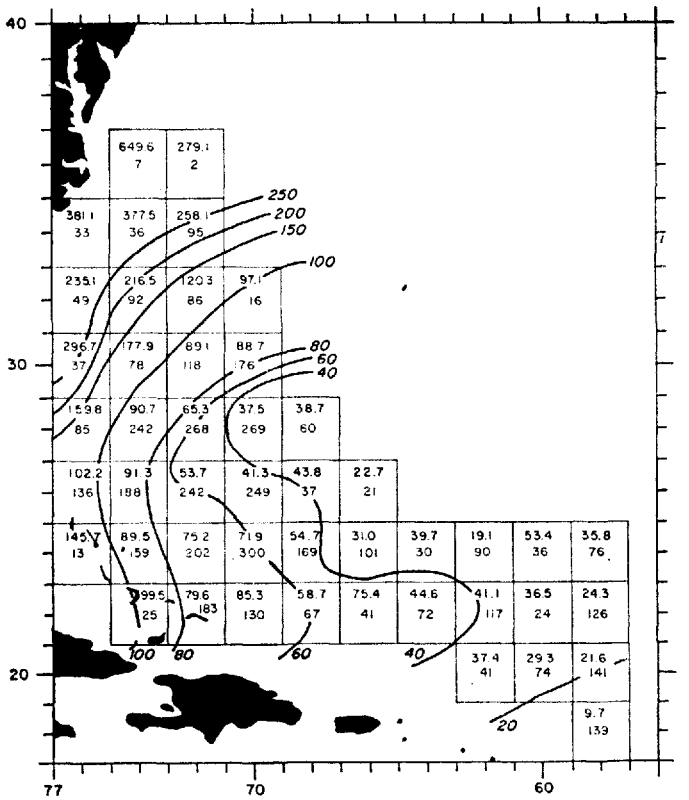

Figure 3. Contours of total kinetic energy in ergs/g at 700 m computed from the data shown in Figure 2. In each box the upper number indicates the average total kinetic energy in the box and the lower number gives the total number of daily samples. North of 31N a few trajectories from Rossby (1982) are used in the estimates of kinetic energy but are not shown in Figure 2.

may be a region where locally the kinetic energy is at a minimum. The reason for this apparent local minimum is not clear, though FRR did see a similar local minimum at 1500 m in the MODE SOFAR float data from the same region and ascribed it to a combination of the effects of boundaries and topographic relief. As will be seen, this local minimum is also present in the POLYMODE 2000 m float data.

With some degree of uncertainty, the geographical variability of the mean field may be estimated from the 700 m data set; however, the coverage of data is not sufficient to resolve the mean with any statistical confidence over squares as small as two degrees on a side. Moreover, given the amount and distribution of data at 700 m, only the coarsest spatial averaging can be used for estimating the mean with any degree of confidence. For purposes of estimating the mean, the western North

Table 3. Estimates of the mean velocity at 700 m, averaged over 12° squares. Error bounds represent two standard deviations of the mean estimate. Subscripts 1 and 2 denote east and north components.

Region	Area	Number of daily observations	$\bar{u}_1$ (cm/sec)	$\bar{u}_2$ (cm/sec)
1	29-41N 67-79W	824	$-.32 \pm 2.2$	1.7 ± 2.9
2	17-29N 67-79W	3542	$-.47 \pm 1.3$	$-.76 \pm 1.5$
3	17-29N 55-67W	941	4.0 ± 2.2	$-.42 \pm 1.2$

Atlantic has been divided into 12° by 12° squares, yielding estimates in three distinct regions of the basin.

The three regions used in this averaging procedure are not entirely arbitrary and coincide loosely with distinct regions of the spaghetti plot. The regions are

(1) 29-41N, 67-79W.
This region includes one long trajectory from the group set prior to the LDE (shown in Fig. 3) and, for statistical purposes, a few shorter trajectories (shown in Rossby, 1982) which were a part of the LDE data set. In general, none of the instruments which entered this region left it to the south, and the northeastern edge of this region often formed the northeastern limit to the tracking system.

(2) 17-29N, 67-79W.
This region includes a large collection of long trajectories, all of which were from floats set prior to the LDE. This region contains mainly instruments which did not move north of the northern boundary of the box but instead moved generally to the south and west.

(3) 17-29N, 55-67W.
This previously unexplored region includes several very long pre-LDE trajectories which exhibit very low frequency (period greater than 200 days) zonal motions, with the bulk of the observations indicating an eastward flow.

The resulting areal mean velocities, with error estimates (see the Appendix for a discussion of these errors) are given in Table 3. Clearly in most instances the mean estimates cannot be bounded away from zero at the 95% level. However, in several cases the computed means do seem plausible, even if no rigorous statistical significance can be claimed. In Region 1, in the northwest corner, there appears to be a northwestward mean which is consistent with classical ideas of entrainment into the Gulf to the north of Cape Hatteras (Worthington, 1976). Both the direction and speed of the estimated mean flow in Region 2 at 700 m are remarkably similar to those determined by FRR from the MODE float data at 1500 m. The

means computed for these first two regions are consistent with the qualitative idea mentioned earlier that there is little mean particle exchange occurring across the region 29-31N in the western North Atlantic at this depth.

In Region 3, in the southeast corner, the estimates of the mean are the most intriguing of all. The meridional mean is small and cannot be bounded away from zero. However, the zonal mean is surprisingly large, 4 cm sec^{-1} to the *east*, with an estimated two standard deviation error of 2.2 cm sec^{-1}. The data from Region 3 represent largely independent samples, taken over a period longer than three years in a sizeable region of the western North Atlantic, and the eastward flow shows remarkable persistence over this time. While such a mean flow would conflict with the classical idea of a single, large, anticyclonic gyre, some recent studies (Reid, 1978; Wunsch, 1978) have suggested the possibility of the existence of a cyclonic gyre south of the main recirculation region of Worthington (1976), and the mean estimated here may be a manifestation of such a gyre.

We can investigate the spatial partition of the eddy portion of the kinetic energy of the trajectories shown in Figure 2 by applying the *F*-test (Snedecor and Cochran, 1967) to the observations. Once the mean velocity field for each region is removed from the trajectory data, it is found that the resulting ratios of zonal to meridional eddy kinetic energy are not statistically different from 1 in any of the three regions, at 80% significance. The ratio is 1.3 in Region 1 (with 11 and 19 degrees of freedom in the zonal and meridional directions), 1.1 in Region 2 (49 and 81 degrees of freedom) and 1.2 in Region 3 (11 and 25 degrees of freedom); the details of these computations are given in the Appendix. Thus, when averaged over all the eddies, there appears to be equipartition of zonal and meridional components of the eddy energy. In any particular range of periods, however, one of these components may significantly exceed the other. As will be shown in following sections, for example, in the thermocline the zonal eddy energy appears at longer time scales than the meridional. When these eddy quantities are added to the differing mean flows for the different regions, the trajectories can take on quite different regional characteristics, as is evident in Figure 2.

b. 2000 m data. At 2000 m, the data coverage of the western North Atlantic is less dense than at 700 m. The spaghetti plot of all 2000 m data, shown in Figure 4, includes trajectories from 6 different instruments, varying in length from 531 to 1047 days.

At this level the effects of bottom topography are evident in the trajectories, though the instruments themselves are usually more than 3000 m above the local bottom. The presence of the Blake-Bahama Outer Ridge near the western boundary appears to be influencing the character of motion a great deal—two instruments moved along its flanks in a northwest/southeast fashion for a time, and one eventually continued west to the Blake Escarpment before moving south along the edge

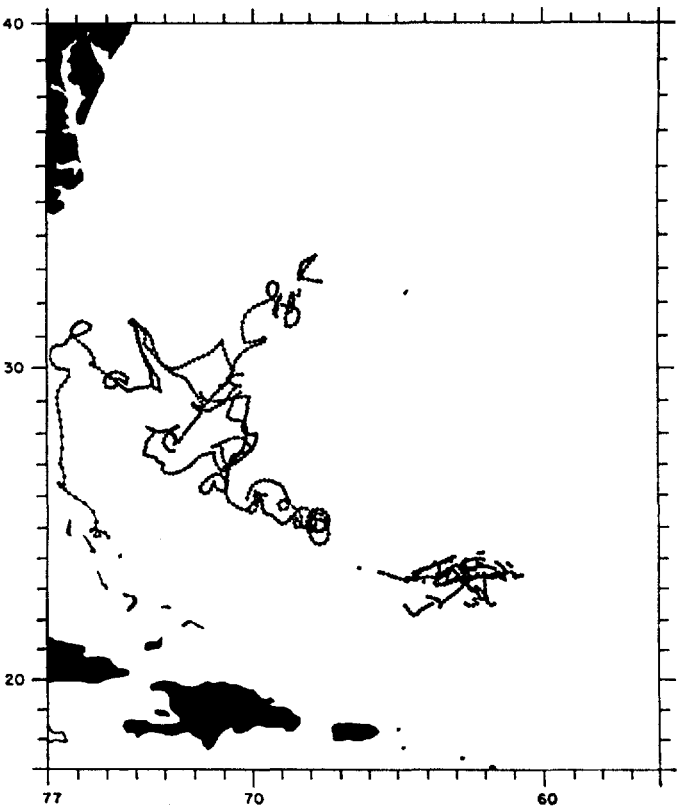

Figure 4. As for Figure 2, but for 2000 m.

of the escarpment. This trajectory was nearly the same as those described by Riser *et al.* (1978) from the MODE float data. Other characteristics of the MODE data obtain as well: in general, instruments do not penetrate the area of the Blake Basin (26-30N, 74-76W) except in the manner noted above, suggesting that the steep bottom slopes in the region effectively block the westward motion of the fluid below the thermocline. In addition, as with both the MODE float data at 1500 m and the 700 m data previously discussed, there is little tendency for any of the floats to penetrate the region north of 31N; all but one of the instruments at this level were set south of 31N, and none of the instruments showed a net drift to the north over its lifetime.

In the southeastern corner of the composite diagram, there are three trajectories which result from the Nares Abyssal Plain launch of March, 1976. All three instruments were set at the same point and continued to be tracked through April, 1978. Over this period the trajectories indicate only very weak relative dispersion, and often the floats moved at extremely low speeds for considerable periods; the speeds

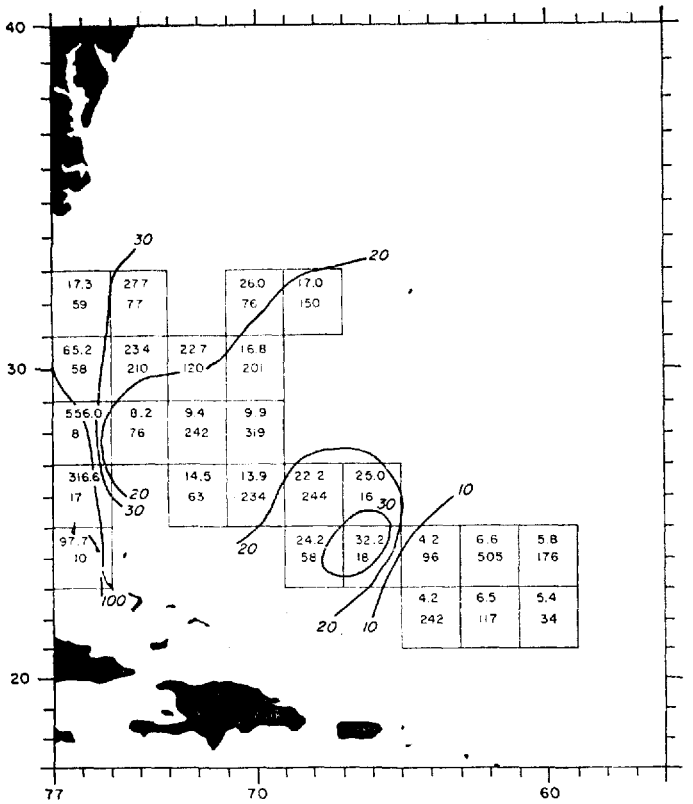

Figure 5. As for Figure 3, but for 2000 m.

are infrequently comparable to their more western counterparts, and the actual displacements of particles in the Nares area appear to be considerably less than for particles nearer the western boundary.

In Figure 5 total kinetic energy computed from the 2000 m data is shown. As with the 700 m data, there is an increase from east to west, especially very near the western boundary, though there are rather marked qualitative differences between the deep and shallow levels. Once again, the greater MODE area (28N, 71W) appears to be a region of a local kinetic energy minimum. This agrees with the results of FRR for the 1500 m MODE floats; the kinetic energy levels at 2000 m appear to be slightly higher than the results from 1500 m in their study. Southeast of the MODE region, there is a region of a local kinetic energy maximum, with local energy levels higher than anywhere else in the sampled area except for the extreme western boundary area. This is also the region of roughest bottom topography in the entire sample region, the other areas being largely abyssal plains except very near the boundaries, which might suggest that the local increase in kinetic

Table 4. Estimates of the mean velocity at 2000 m, averaged east and west of 67W. Error bounds represent two standard deviations of the mean estimate. Subscripts 1 and 2 denote east and north components.

Region	Area	Number of daily observations	$\bar{u}_1$ (cm/sec)	$\bar{u}_2$ (cm/sec)
1	17-40N 67-79W	2333	$-.40 \pm .53$	$-.60 \pm .56$
2	17-40N 55-67W	1198	$-.30 \pm .84$	$-.30 \pm .43$

energy may be due to bottom generated variability. However, all of the data in this region are from the long drift of a single instrument, so this may not be representative of the mean total kinetic energy in this area. Southeast of this region, in the vicinity of the Nares Abyssal Plain, the local kinetic energy levels are the lowest of any in the area of study, perhaps typical of the deep ocean far away from boundaries and major topographic features.

Estimates of the mean velocity at 2000 m are given in Table 4. For estimating the mean, we have divided the 2000 m data into two groups, one on either side of 67W. In the data west of 67W, both the northward and eastward estimated means are negative, and the values for the estimated errors of the mean hint that at least the sign of the estimated means in this region are correct. Moreover, the southwestward mean estimated here at 2000 m $((\bar{u}_1, \bar{u}_2) = (-.4, -.6)$ cm sec$^{-1})$ is not unlike that found by FRR from the MODE 1500 m float data set $((\bar{u}_1, \bar{u}_2) = (-.9, -.3)$ cm sec$^{-1})$, and also not unlike that found in the 700 m POLYMODE float data (the subscripts 1 and 2 indicate the zonal and meridional velocity components, and the overbar denotes an areal average). The estimated mean flow east of 67W is also to the south.

While the standard errors in estimating the 2000 m mean velocity field from the float data are not small in either of the two abyssal regions considered here, the mean estimates presented here are consistent with recent indirect estimates of the mean flow inferred from geochemical tracer distributions (Jenkins and Rhines, 1980) and with the data syntheses of Worthington (1976) and Wunsch (1978), and such a southerly mean at depth in the western North Atlantic is also the central prediction of Stommel's (1958) abyssal circulation model.

We can investigate the partition of eddy zonal and meridional kinetic energies at 2000 m by using the *F*-test. West of 67W, we find that the meridional eddy kinetic energy exceeds the zonal at the 80% level (the ratio of meridional to zonal being 1.5, with 65 and 61 degrees of freedom in the zonal and meridional directions). This suggests that fluid parcels in this region may preferentially oscillate along topographic contours, since west of 67W the large scale topography generally runs north-south. East of 67W, where the bottom is very flat, the zonal eddy kinetic

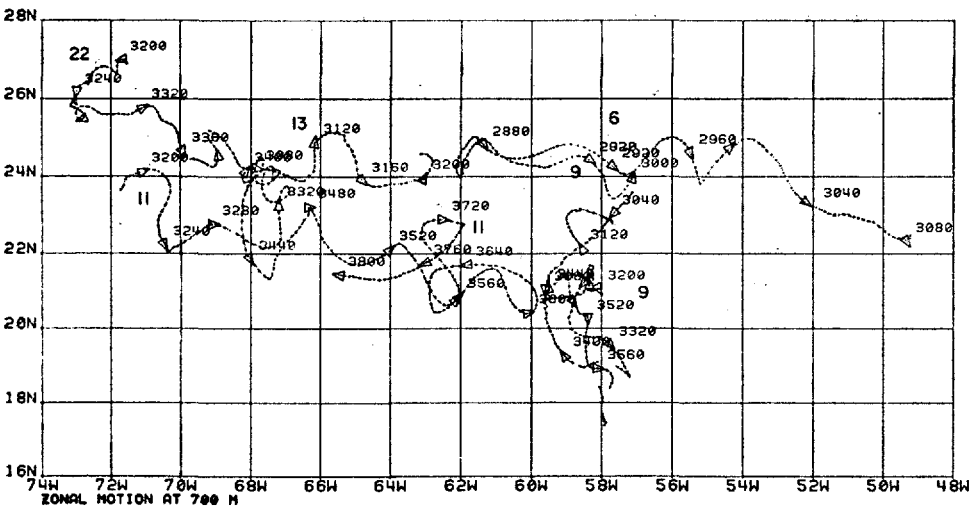

Figure 6. Floats 6, 9, 11, 13, and 22, at 700 m. Three fixes per day are shown. Larger dot is the first fix of the day. Arrows denote direction of motion along the trajectory. Numbers to the upper right of the arrows denote time at the arrow in modified Julian days (see Table 2 for conversion to calendar time). Short gaps have been linearly interpolated.

energy exceeds the meridional at the 80% level (the ratio being 1.7, with 16 and 33 degrees of freedom).

3. Zonal flow in the subtropical thermocline

The spaghetti plot of the 700 m data, shown in Figure 2, indicates that over long times, away from the immediate vicinity of the western boundary, the net zonal displacements of particles exceed the net meridional displacements. This is especially true in the southeastern corner of the figure (Region 3, 17-29N, 55-67W in the above discussion of mean flow). Moreover, the estimated mean flow is to the east, 4 ± 2.2 cm sec^{-1}, in this region from the 700 m float data available. The trajectories of 700 m floats 6, 9, 11, 13, and 22, in Figure 6, each show a period of sustained zonal motion ranging in length from 100 to 300 days; a summary of these trajectories and those mentioned in following sections is given in Table 5. With each of these five trajectories the motion was generally eastward, and there is no similar trend in the 700 m data shown in Figure 1 for sustained westward motion. The zonal (eastward) portions of these trajectories are from a rather narrow band of latitudes (22-26N) and extend from nearly the effective western boundary of the basin, 73W, to the western slopes of the Mid-Atlantic Ridge, 49W.

From west to east and north to south, these observations may be summarized as follows. Float 22, set in January, 1977, moved initially southwest, and then moved east for over 100 days before being recovered. Float 13, set in October,

Table 5. Launch and duration information for all floats set prior to December 31, 1977.

Float	Nominal depth (m)	Start day	Last tracked	Duration of trajectory (days)
1	2000	2680	3900	1220
6	700	2840	3080	240
7	2000	2844	3590	746
8	2000	2844	3620	776
9	700	2843	3672	829
10	2000	2844	3509	665
11	700	3051	3800	749
12	850	3054	3510	456
13	700	3051	3230	179
14	700	3052	3630	578
15	700	3051	3060	9
16	700	3056	3086	30
21	700	3166	3729	563
22	700	3170	3365	195
25	700	3251	3900	649
26	700	3251	3800	549
27	2000	3239	3819	580
29	2000	3248	3982	734
30	650	3418	3835	417

1976, moved east for 150 days before it ceased signalling. It was set as part of a group of six instruments which was intended to study an intense lens of Mediterranean water in the southwestern Sargasso Sea (McDowell and Rossby, 1978). The float broke away from the other floats in the group and was the only trajectory of that group to show the zonal motion immediately. Floats 6 and 9 were set in March, 1976 in the Nares Abyssal Plain area, and both initially moved east in a generally zonal fashion. Due to technical problems with the receiving system at two of the islands, after about 100 days float 9 was no longer trackable. However, it reappeared 30 days later moving southwest, and over the next three years continued to oscillate from north to south along 59W with no further evidence of sustained zonal motion. Float 6 continued to move east to 49W, over the flanks of the Mid-Atlantic Ridge, before finally moving out of tracking range. Float 11, set with float 13 in the Mediterranean lens study, initially followed the lens but later broke away and moved generally to the east along 22N for nearly 400 days. In the vicinity of 21N, 60W, it turned back to the west and moved in that direction for approximately 200 days before ceasing operation.

With each of these trajectories there are often meridional particle oscillations superimposed upon the long term zonal drift. With floats 6 and 13 and the first part of float 9, the meridional oscillation has a period of approximately 60 days. Similarly, with float 11, there are oscillations with Lagrangian periods of 40-80 days present superimposed upon the zonal flow, and in some instances (days 3320-3440

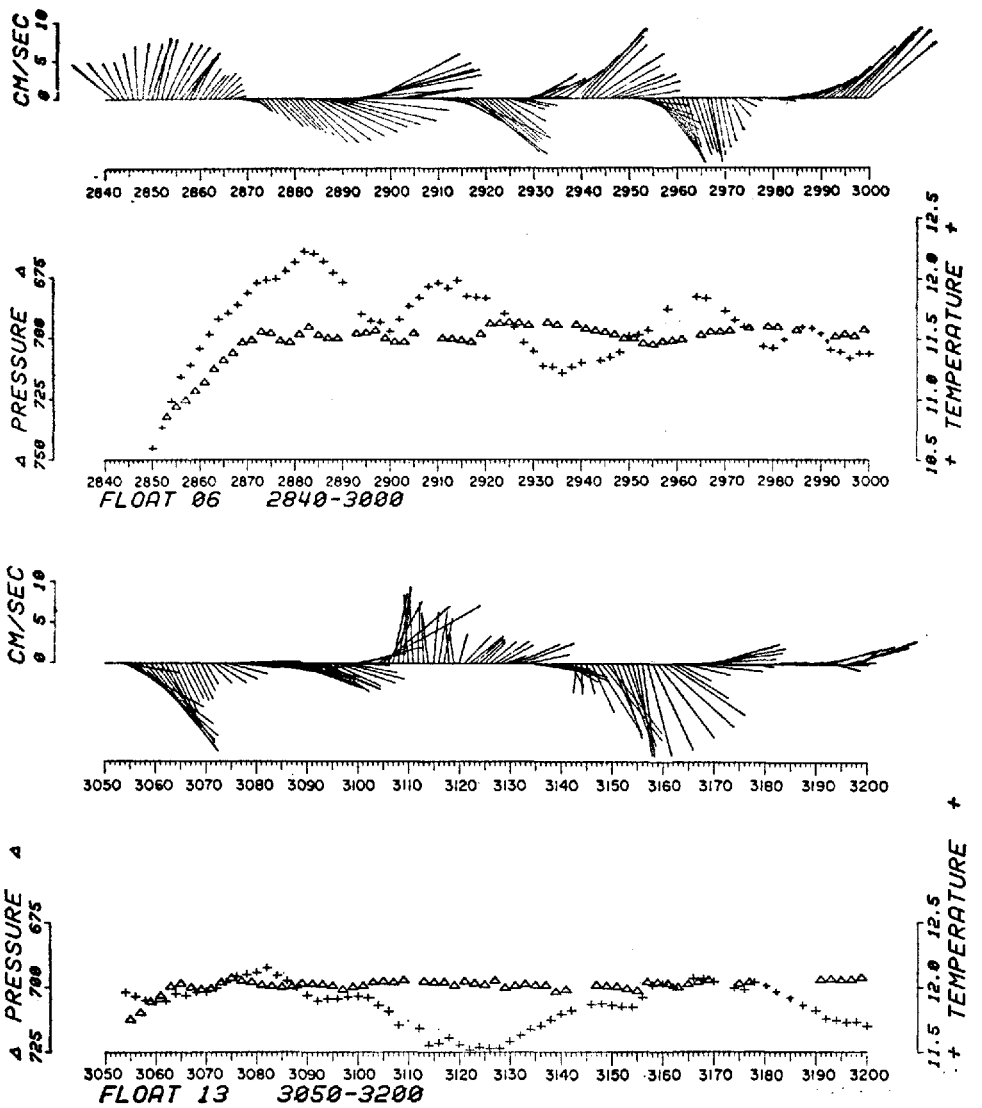

Figure 7. (a) Stick plot of velocity, and temperature and pressure telemetry from float 6, days 2840-3000. On the stick plot, north is up and east is to the right. Velocities are smoothed over 5 days. Presures and temperatures represent 2 day running means. (b) As for (a), but for float 13.

for example) an even faster mode of oscillation appears. The second part of float 9, along 59W, contains slower meridional oscillations (period over 200 days) with a weak or nonexistent long term zonal flow. Some of these characteristics are present in the temperature measured along trajectories as well (Fig. 7). Clearly the north-

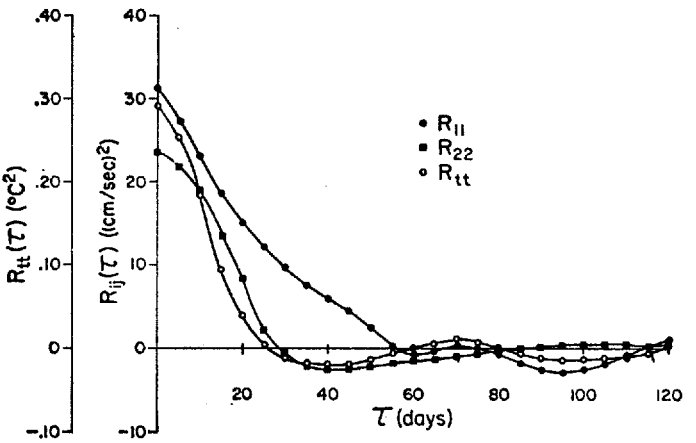

Figure 8. Temporal autocovariances computed as defined in text from the ensemble of floats shown in Figure 6. Subscript 1 denotes the east component, 2 denotes the north component, t denotes the temperature.

south oscillations are often accompanied by apparently phase locked changes in temperature (float 13 for example), though at other times the temperature does not change in phase with the displacement, as with float 6; the dynamical implications of such behavior are discused in detail in Riser (1982b).

From the trajectories shown in Figure 6, it is possible to estimate the Lagrangian covariance tensor, a quantity that is intimately related to the diffusivity of the eddies in the field (Taylor, 1921). Let the covariance tensor R be defined by

$$R_{ij}(\tau) = < \frac{1}{T} \int_{t_o}^{t_o + T} u_i(\mathbf{x}_0, t)\, u_j(\mathbf{x}_0, t+\tau)\, dt >$$

where $\mathbf{x}_0$ and t_0 are the initial space and time coordinates for a fluid parcel and T is the time over which the parcel is being observed. The angled brackets denote the average over an ensemble of such fluid parcels. The velocities u_i (again, $i = 1$ or 2 for zonal or meridional components) in the integral are perturbation quantities; for the trajectories shown in Figure 6 the mean velocity from Region 3 has been removed from the trajectories before computing the autocovariance. The resulting autocovariance functions for the data shown in Figure 6 are shown in Figure 8. The first zero crossings of these functions, at 29 and 57 days for the meridional and zonal autocovariances, respectively, are one measure of the characteristic time scales of the sampled processes in this region. A more conventional measure of the characteristic time scales can be defined by examining the tensor I, whose diagonal elements are given by

$$I_{ii} = <u_i^2>^{-1} \int_0^{T_\tau} R_{ii}(\tau)\, d\tau$$

where T_τ is a time over which the ensemble is observed. For $T_\tau \sim 0$, then $I_{ii} \sim T_\tau$ since R_{ii} is very nearly $\langle u_i^2 \rangle$ at small lags. Alternatively, as $T_\tau \to \infty$, the integral of R_{ii} should reach some nearly constant value, and I_{ii} will approach a constant. We shall refer to this value of I_{ii} as $T_\tau \to \infty$ as the Lagrangian integral time scale (Taylor, 1921). For the autocovariances shown in Figure 8, the integral time scales for the zonal and meridional velocities are 18 and 7 days. Both the zonal and the meridional covariances lack the deep negative side lobes characteristic of a field of only a very few Fourier components, indicating a broad spectrum of motions. Clearly this is the case for the individual trajectories of floats 9 and 11. For other members of the ensemble, however, the reverse may be true, as with the seemingly simple oscillations present in the trajectory of float 6 (and to a lesser extent float 13) which are surprisingly persistent over several periods.

Also shown in Figure 8 is the autocovariance function of the quasi-Lagrangian temperature for the five trajectories. In this and other examples of the 700 m temperature autocovariance discussed herein, the mean temperature field has been removed by fitting a quadratic surface to the 700 m averaged temperature for the western North Atlantic given by Lai and Richardson (1977) and then by removing this spatially varying mean from each trajectory (discussed in the Appendix). The temperature autocovariance is qualitatively more similar to that of meridional velocity than zonal velocity and has a Lagrangian integral time scale of 8 days, similar to the result for meridional velocity; over all of the trajectories shown in Figure 6, the correlation coefficient between temperature and meridional displacement is $-.5$ and is significant at the 90% level. The Lagrangian time scales estimated above for both velocity and temperature are not unlike those estimated by Richman *et al.* (1977) from the long term 500 m Eulerian data collected during and after MODE in the sense that the zonal velocity time scale is considerably longer than the meridional time scale. Thus, qualitatively, both the previous Eulerian measurements and Lagrangian observations reported here point to an ubiquity of long period zonal eddy motion in the thermocline in the region south of the Gulf Stream recirculation.

From the computed covariances, some measure of the effective diffusivity can be obtained. As was shown by Taylor (1921), if the velocity variance and integral time scale of an ensemble of fluid parcels are known, then the diagonal elements of the diffusivity tensor κ are given by

$$\kappa_{ii} = I_{ii}\langle u_i^2 \rangle = \int_0^{T_\tau} R_{ii}(\tau)\, d\tau$$

in the limit of $T_\tau \to \infty$. In this context, the quantity κ_{ii} represents essentially the diffusive effects of mesoscale eddies on the mean field. From the autocovariances of horizonal velocities computed above we find $(\kappa_{11}, \kappa_{22}) = ((4.5,1.8)\times 10^7)$ cm^2 sec^{-1}, values below classical estimates of the eddy diffusivities in a large scale ocean

(Sverdrup *et al.*, 1942), though larger than values computed for the MODE region (FRR) at 1500 m. Considering the possible errors in estimating the integral time scale and the velocity variance, the errors in these diffusivity estimates may be as large as ±50% of the estimates themselves. Nonetheless, given the nature of the trajectories used in this computation (especially the long zonal time scale), it does not seem unreasonable that the zonal diffusivity should exceed the meridional. From a mechanistic point of view, such zonal anisotropies in particle motion may place severe constraints on the distribution of heat, salt, and nutrients in the upper ocean, and might partially explain the tendency for these fields often to show greater meridional than zonal contrasts over large distances in the mid-ocean.

4. Deep circulation in the Nares Abyssal Plain region

In conjunction with the setting of floats 6 and 9, at 700 m, three instruments at 2000 m, floats 7, 8 and 10, were also set at the same location. In addition, a mooring with current meters at 1500 m and 2000 m was set near the launch positions.

Trajectories of floats 7 and 8, shown in Figure 9, indicate that for over two years the instruments remained within two degrees of their initial position. However, in addition to the rather low speeds evident in these tracks and the small net movement away from their initial position, what is remarkable about these trajectories is the similarity between them over the two year span: the floats separate only extremely slowly. Some features may be seen nearly simultaneously in both tracks, even at long times after the launch. Both trajectories change from a southwest to a nearly due east direction around day 2940, nearly 100 days after being set; both show a cyclonic loop beginning around day 3040; around day 3100 both trajectories turn back to the east; near day 3200, both instruments reach their easternmost point and then begin moving northwest. Finally, after day 3220 the floats show some small degree of relative separation, though by day 3400 both instruments are still near each other in the vicinity of 22.5N, 61W, apparently turning to the northwest. Both change direction from southwest to northeast near day 3540 and eventually move to the vicinity of 23N, 63W before the tracking effectively ceased in April, 1978. Float 10, not shown here, is a considerably gappier record, but its trajectory is qualitatively similar to those of floats 7 and 8.

The similarity of these trajectories over such long times suggests that the predominant energy containing scale of the abyssal waters in this region may be larger than the distance between the instruments—a distance, at times, such as around day 3400, as large as 100 km. This stands in striking contrast to the MODE region, for which it has been suggested (the MODE Group, 1978) that the dominant energy containing scale is around 50 km. But here, in the Nares region, it is quite common that the floats are at least 50 km apart, yet over two years even the details of their motion are virtually the same. As with the shallower trajectories in

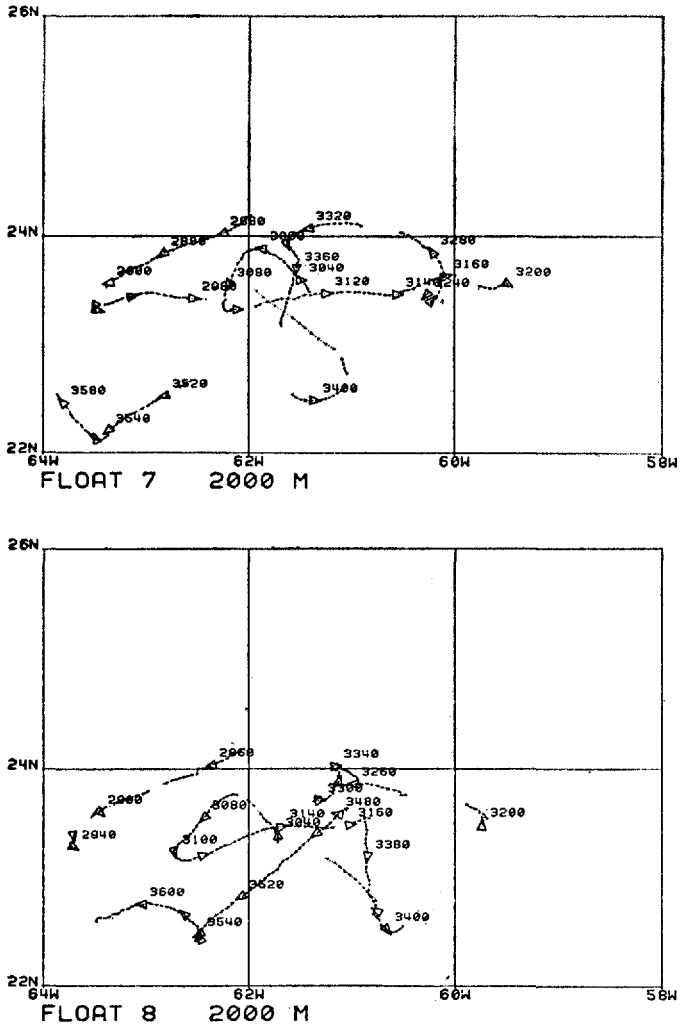

Figure 9. (a) Float 7, at 2000 m. Three fixes per day are shown; the larger dot represents the first fix of the day. Arrows denote direction of motion along the trajectory. Numbers to the upper right of the arrow denote time at the arrow in modified Julian days. Gaps denote missing data. (b) Float 8, at 2000 m.

this region, it appears that at the longest time scales zonal motions are dominant, though there is some higher frequency motion present in meridional motions. Float 7, for example, nearly returns to its initial position after undergoing one largely zonal oscillation over a period of about 480 days.

Autocovariance functions computed from horizontal velocities from floats 7, 8, and 10, shown in Figure 10, are not unlike those shown by FRR for the MODE

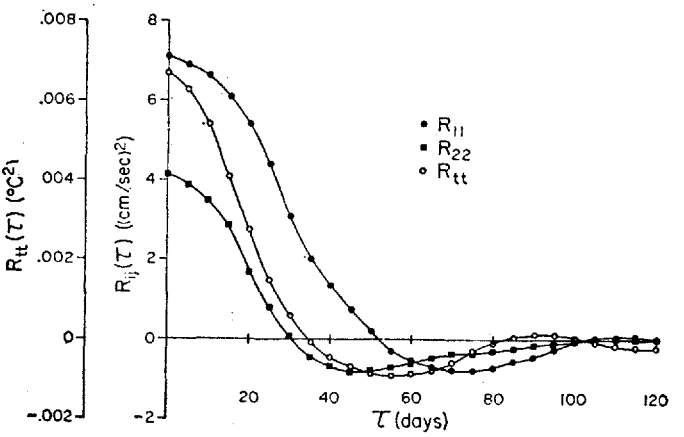

Figure 10. Temporal autocovariances from the ensemble composed of floats 7, 8, and 10.

floats, though the actual magnitudes of the functions for the deep Nares floats are less than for the MODE data; this simply reflects the lower energies present in the Nares region (the mean velocities removed are the values given for Region 2 in Table 4). The Lagrangian integral time scales are 15 and 7 days for the zonal and meridional velocities. For quasi-Lagrangian temperature, the time scale is 9 days (the mean temperature removed from the data is simply taken as the ensemble mean over the trajectories of floats 7, 8, and 10 since there is little historical data from this region at 2000 m, and hence spatial variations in the mean temperature field cannot be well estimated). The zonal integral time scale estimated here for the Nares area is thus slightly higher than the 12 day estimate from the MODE 1500 m floats (FRR). The temperature, while similar to the meridional velocity in time scale, is uncorrelated with both zonal and meridional displacements, as might be expected at this level of the water column whenever the low-frequency vertical structure is more complex than just a single eigenmode. The Lagrangian diffusivities estimated from these trajectories are $(\kappa_{11}, \kappa_{22}) = ((9.0, 2.6) \times 10^6)$ cm² sec^{-1}, values comparable to those of the MODE region at 1500 m (FRR) though the lowest of any of the regions in the present study; perhaps this region is "typical" of true mid-ocean conditions at depth.

The moored data from the Nares area contributes a different perspective on the deep flow in this region. The progressive vector diagram of low-passed moored velocity from 2000 m is shown in Figure 11 along with the trajectory of float 7 during the same time interval. The velocity of the float and the velocity at the current meter are qualitatively similar (to the southwest) for about 30 days, or until the distance between the two reaches about 40 km. Between day 2880 and 2900 the flow at the mooring swung to the east, while the float trajectory did not change direction until about 35 days later, near day 2920. The motion of the float

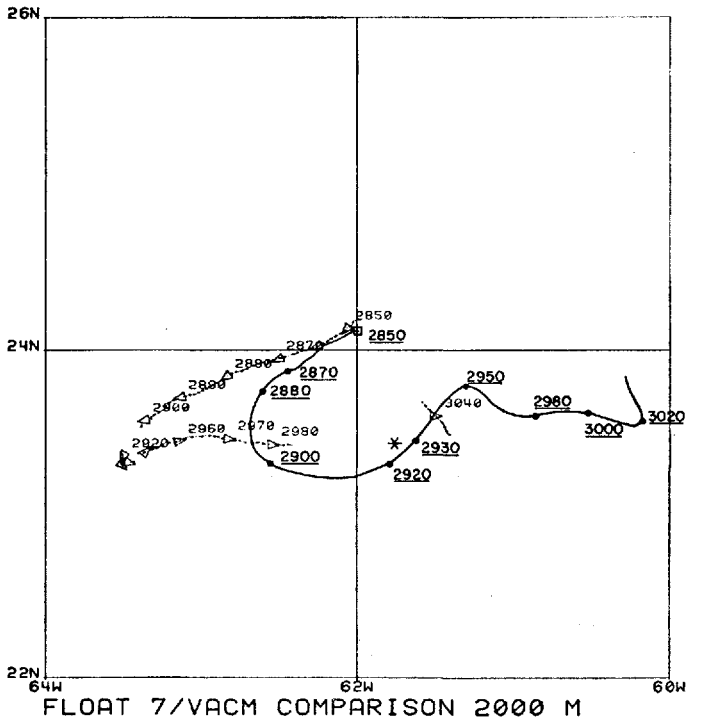

Figure 11. Trajectory of float 7 with progressive vector diagram from 2000 m VACM superimposed as if it were a trajectory. Float trajectory is noted by dots, with arrows giving direction of motion along float trajectory. Numbers to the upper right of the arrows give the time at the arrow in modified Julian days. Position of the VACM is given by the symbol ⊡; the progressive vector diagram is the solid line. Underlined numbers along the progressive vector diagram denote the times at the dots in modified Julian days. The symbol * gives the estimated position of float 7 on day 3020.

then also turned eastward. When the southwestward motion at the float ceased, the float was 170 km west of the mooring; the direction change at the mooring preceded that at the float by approximately 35 days. This leads to an estimate of a lower bound of 5.5 cm sec^{-1} for the westward component of the translation speed of this event, an estimate not dissimilar to the westward phase speeds estimated by FRR from the MODE floats. However, while in that study they concluded that the motions at 1500 m were wavelike in character (hence their terminology "phase speed"), we have little supporting evidence that the 2000 m motions in the Nares area are of a wavelike nature. We remark that the root-mean-square particle speed from over two years of float observations at 2000 m here, 2.1 cm sec^{-1}, compared to the translation speed estimated above, yields a lower bound on the wave steepness of .43 if the translation speed is interpreted as a phase speed. This estimate

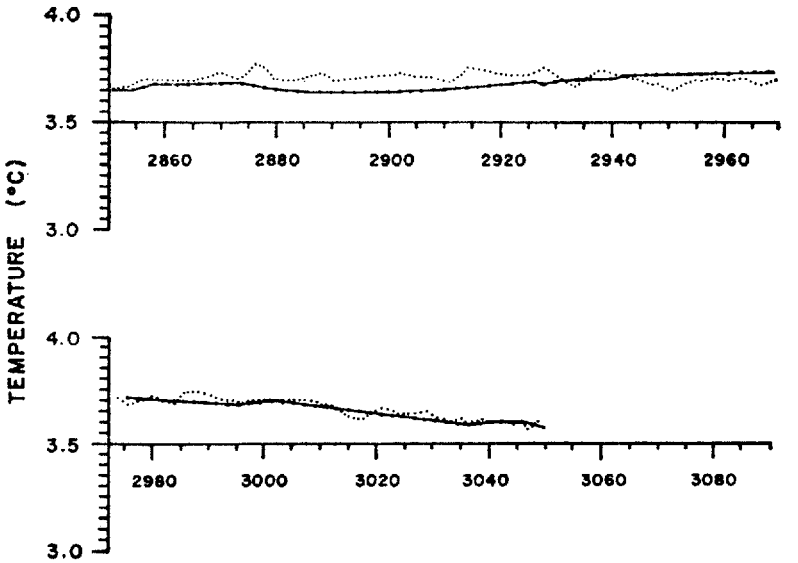

Figure 12. Time series of temperature from float 7 (solid line) at 2000 m and VACM at 2000 m (dashed line). Float temperatures are computed on board the float as 2 day running means. For purposes of comparison, VACM temperatures have been computed in the same manner from the original 15 minute samples.

of nonlinearity is within the range of that estimated from the MODE float data (FRR), and suggests that, even at these reduced energy levels, if these motions are wavelike they are still of a nonlinear nature. The overall similarity between the progressive vector diagram from the 2000 m moored data and the 2000 m float trajectories suggests that the energy containing scales of motion here may be somewhat larger than the distance between the mooring and the floats, a distance sometimes larger than 100 km.

It is also useful to compare the moored and quasi-Lagrangian temperatures from 2000 m. In Figure 12 a time series plot of temperature data from the mooring and float 7 is shown. The two are quite similar, especially during the final 70 days of the comparison. Two essential pieces of information are contained in this pair. First, from days 2970 to 3050, the moored and quasi-Lagrangian temperatures are changing in nearly the same manner, though the float is moving east at approximately 3 cm sec^{-1} during this period and is as far as 100 km away from the mooring throughout this time span. This uniform temperature decrease implies that at this depth isotherms are shoaling in time (vertical velocity is up) rather uniformly over spatial scales considerably larger than the Rossby radius of deformation in these waters. Thus the temperature field quite independently shows the relatively long spatial scales alluded to earlier in the discussion of moored and quasi-Lagrangian velocity data. The second comparison of these two temperature data sets con-

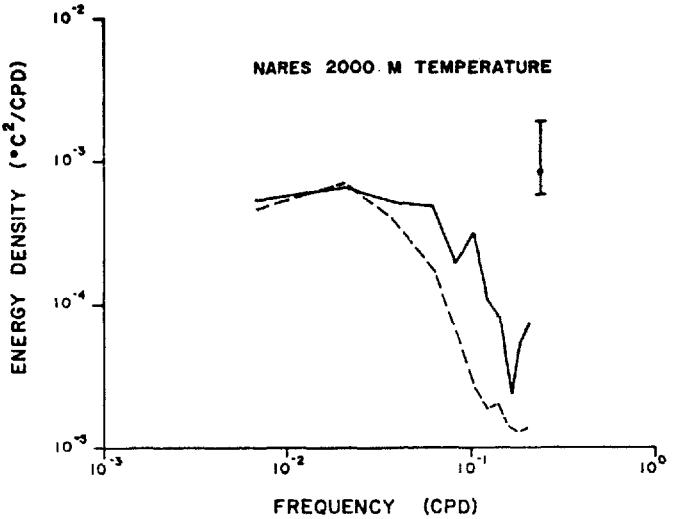

Figure 13. Temperature spectra from float 7 (dashed line) at 2000 m and VACM at 2000 m (solid line) located at 24°03'N, 61°59'W. Error bar gives approximate 95% confidence limits for 10 degrees of freedom. Data from days 2840-2980 have been used for both estimates.

cerns the higher frequency content: there is considerably more variability at periods of 5-20 days in the Eulerian record than in the quasi-Lagrangian one. The spectra of these records, shown in Figure 16, indicate that at periods of 5-30 days, the variance of the Eulerian temperature record is 3-5 times that of the quasi-Lagrangian one, though at the longest periods resolvable the spectra are nearly identical.

The excess variance in the Eulerian temperature record compared to the quasi-Lagrangian record is not unanticipated. The difference at the higher temporal frequencies is very likely the result of advection of spatial variability past the fixed sensor, thus accounting for the apparent temporal variability. In the quasi-Lagrangian frame, however, the instrument moves with the advected flow (and the higher wavenumber structure), and hence no corresponding temporal variability appears. FRR found a similar result in comparing quasi-Lagrangian and Eulerian kinetic energy spectra from the MODE region and speculated that this spectral difference may be a general property of kinetic energy spectra measured in these differing reference frames.

5. Motions in the thermocline in a near boundary region and over the Hatteras Abyssal Plain

In the thermocline south and east of the greater MODE region, it has been shown that the combination of long zonal eddy time scales and relatively strong zonal mean flows result in large net zonal particle displacements, at least on the

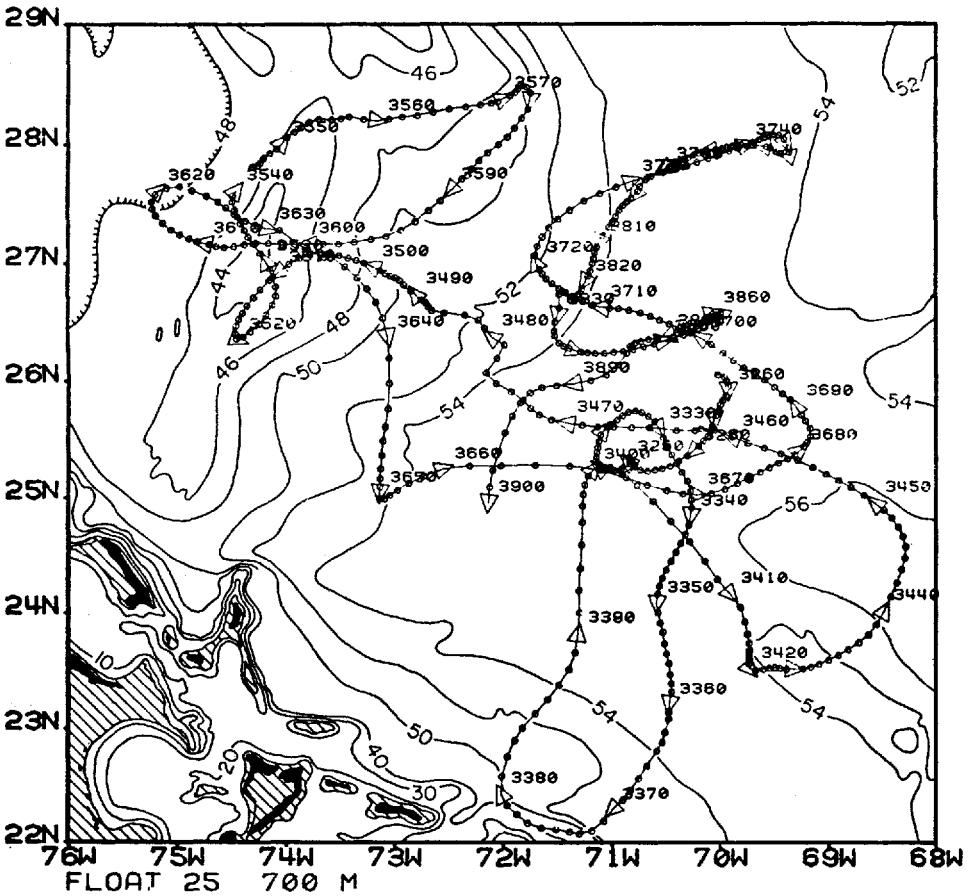

Figure 14. Trajectory of float 25, at 700 m, superimposed on bottom topography of Pratt (1968). Bottom contours are in hundreds of meters. Open circles give the first fix of each day. Arrows denote direction of motion along the trajectory. Numbers to the upper right of the arrows denote the time at the arrow in modified Julian days.

time scales that data have been collected so far. Nearer the western boundary and farther to the north, however, this is generally not the case, as is illustrated by the trajectories of two instruments, floats 25 and 30, shown in Figures 14 and 15.

Over a time of 650 days, float 25 covered a sizeable area of the western North Atlantic, though its net displacement over that time was only 200 km. Its motion was generally not of an organized sort, as was the case with some of the 700 m trajectories from farther east, but instead seemed to be almost a random walk type of behavior around 25°30′N, 71W. There are, however, some periods when the motion was rather regular; from days 3520-3600 and again from days 3710-3830 and 3839-3895 there were regular oscillations southwest to northeast and back

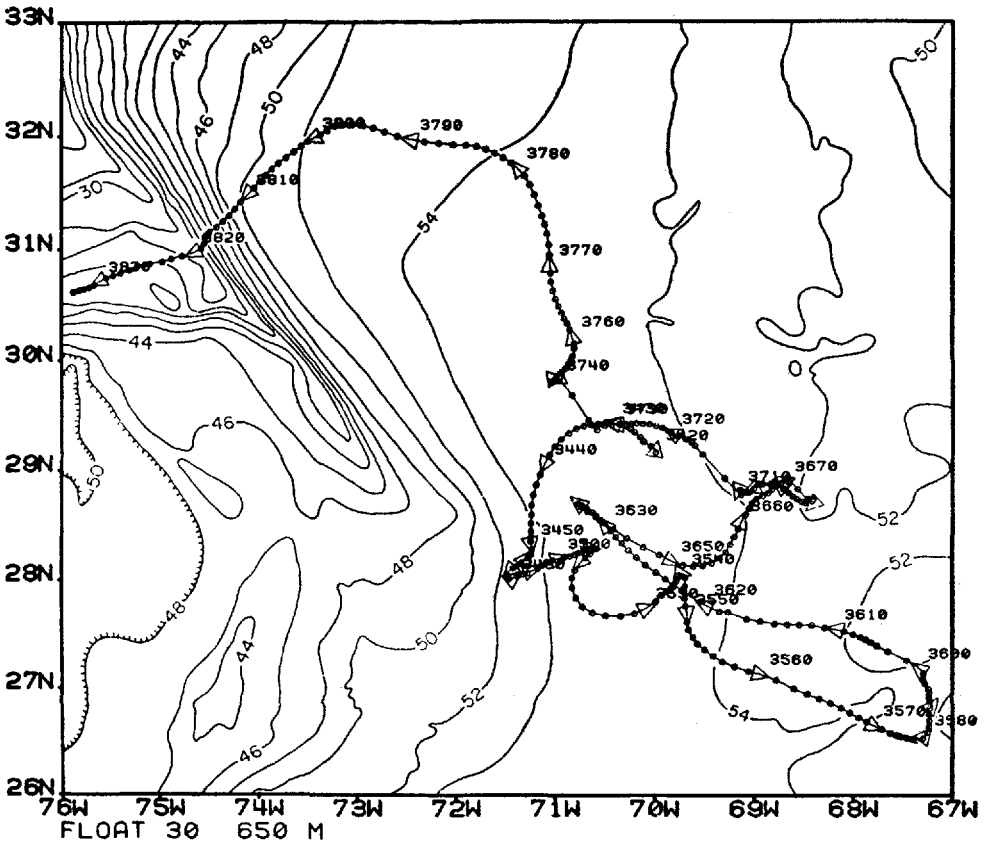

Figure 15. As for Figure 14, but for float 30, at 650 m.

again. While the southernmost portions of this trajectory (for example, near days 3380, 3650, and 3520) are within 100 km of the southwestern boundary of the basin, the Bahamas and Lesser Antilles, there is no evidence of a persistent "Antilles Current"; the transient motions in this near boundary region are apparently far stronger than any mean flows.

During the first year of the trajectory of float 30, three degrees farther to the north and at 650 m, there is similar behavior: there are large amplitude oscillations around a centroid of 28°30'N, 70W. The trajectory changed abruptly around day 3730, when the instrument began to break way to the northwest, and the motion accelerated.

In Figure 16 temporal autocovariance functions computed from the trajectories of these two floats and their temperatures are shown, with mean velocities from Region 2 removed from the data. For float 30, the autocovariances were computed from the data from before day 3730, when the float broke away to the northwest.

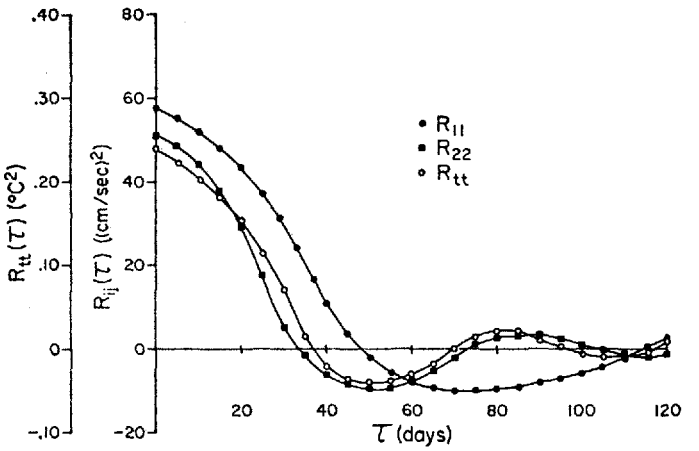

Figure 16. Temporal autocovariances from the ensemble composed of floats 25 and 30, computed as described in text.

Each instrument thus remains in a region of relatively homogeneous statistics (Fig. 3) during the interval used to estimate the autocovariance. The averaged autocovariance for the two trajectories indicates that, as before, the zonal time scale is longer than the meridional, and the quasi-Lagrangian temperature time scale is similar to that for meridional velocity. The integral time scales for zonal velocity, meridional velocity, and temperature are 13 days, 8 days, and 8 days, respectively. While the zonal time scale is longer than the meridional or the temperature time scale, it is shorter than that for particles in the region to the southeast of the greater MODE region. Richman *et al.* (1977), from Eulerian data, also noted longer zonal than meridional time scales in the thermocline in the MODE region.

This pair of 700 m trajectories from the greater MODE region suggests the possibility of particle residence times of 1 to 3 years in this region of the western North Atlantic, though float observations after the LDE (Rossby, 1982) indicate that some particles may remain in this region for shorter times before being entrained into the Gulf Stream. Based on these two trajectories, the conclusion might be drawn that the greater MODE region is not, on a time averaged basis, an area of particularly vigorous horizontal exchange of particles. The Lagrangian eddy diffusivities associated with the autocovariances shown in Figure 16 are $(\kappa_{11}, \kappa_{22}) = ((6.5, 3.5)\times 10^7)$ cm^2 sec^{-1}, values which are comparable to the Lagrangian diffusivities computed from the trajectories farther to the southeast.

6. Evidence for recirculation

Only a small portion of the data shown in Figure 2 is from north of 31N. While several instruments set during the LDE did eventually move far north of this lati-

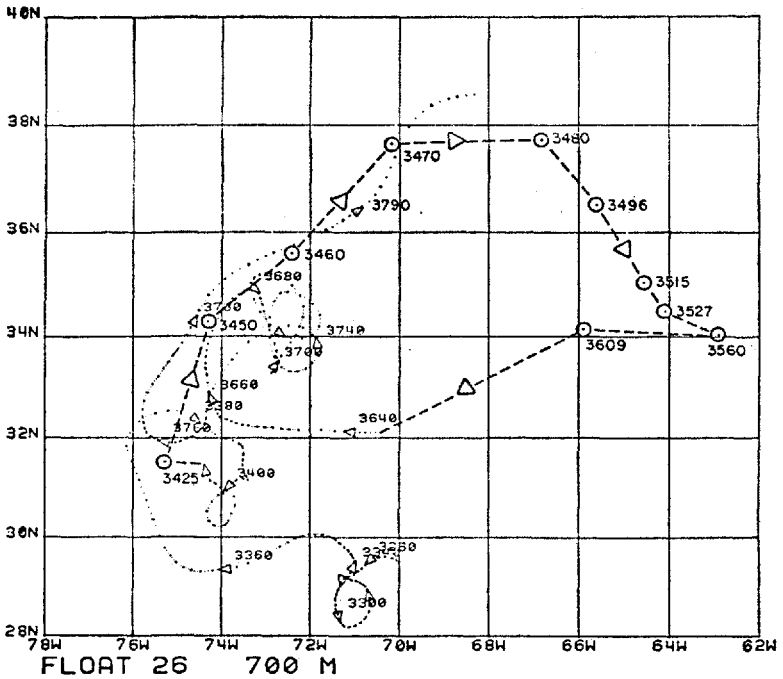

Figure 17. Trajectory of float 26, at 700 m. Before day 3425 and after day 3640 the first fix of each day is shown. Arrows give the direction of motion along the trajectory, and the number to the upper right of the arrow gives the time at the arrow in modified Julian days. Between days 3425 and 3640 intermittent fixes are given by ⊙, connected by dashed lines; arrows give mean direction of motion between these fixes.

tude (Rossby, 1982), it was rare that any of these earlier instruments did so. One instrument, float 26, (shown in Fig. 17) did sample the area to the north of this latitude, and its trajectory provides an example of a mode of circulation in this area not unlike that proposed by Worthington (1976).

Float 26, at 700 m, was set in April, 1977 near 29N, 70W in a rather narrow (50 km), westward flowing, thermocline jet. A 2000 m instrument, float 27, was set at the same time. To summarize, float 26 moved initially west at 5-10 cm sec^{-1} before making a single cyclonic loop to the south. It then continued to the west, accelerating to over 40 cm sec^{-1} near the western boundary approximately 100 days after its initial setting. The float then moved northwest at over 60 cm sec^{-1} before making another loop very similar to the earlier one.

After the second loop in the trajectory, the instrument moved into a region where tracking became very difficult due to low signal to noise ratios and high float speeds. It was possible, however, to continue to track the float intermittently, and these sporadic fixes are also shown in Figure 17. Around day 3425 (October 9, 1977)

the float was caught up in the Gulf Stream as it moved out to sea near Cape Hatteras and continued moving northeast at over 30 cm sec^{-1}. Eventually the motion became more eastward, and finally around day 3480 the trajectory turned to the southeast. The motion slowed considerably, to less than 10 cm sec^{-1}, and near day 3560 (February 21, 1978) the trajectory turned back to the west. The motion continued to be westward and southwestward, and on day 3638 (May 10, 1978) continuous tracking again became possible. During this time the float was moving very rapidly (40 cm sec^{-1}) in a nearly due west direction. By day 3660, float 26 had returned to the general vicinity of the Gulf Stream; this was a time of approximately 240 days since it first entered the stream near the same point. The float then again moved northeast and began a series of loops near 34N, 72°30′W, close to a position reported for a Gulf Stream ring (US Department of Commerce, 1978). Eventually, around day 3760, the float rejoined the stream, and again moved northeast on a path quite similar to its trajectory some 300 days earlier when it first joined the stream. Finally, on day 3795, the float moved out of tracking range for the final time.

Particle motion of the kind shown by the trajectory of float 26 is consistent with the Eulerian circulation shown by Worthington (1976) for the upper (12°-17°C) and middle (7°-12°C) thermocline waters of the western North Atlantic. From historical hydrographic data, he shows an anticyclonic recirculation gyre extending to approximately 40W in both of these layers, with closed streamlines throughout the interior of the recirculation region. In his model, the (mean) motion south of about 35N is all to the west, which seems qualitatively similar to the trajectory shown here.

7. An example of abyssal circulation

Float 27 (Fig 18), set at 2000 m with float 26, at 700 m, also moved initially west in the aforementioned jet, indicating some penetration of this apparently strong current into the abyssal waters. However, within a very short time (10 days) of the setting of float 26, the motion of the two instruments seems to have become uncorrelated. Float 27 remained in the Hatteras Abyssal Plain area for over 200 days; during this time it showed a long term westward motion with some superimposed north-south oscillation. During the first 200 days of its drift, the mean westward translation speed of float 27 was 1.4 cm sec^{-1}.

Around day 3450 the float began to turn northwestward, roughly following the contours of the flanks of the Blake-Bahama Outer Ridge, and near day 3475 the motion turned south, nearly coincident with the 5300 m isobath along the Ridge. About day 3530 the float crossed the tip of the Ridge, turned west, and continued to drift toward the western boundary for the next 200 days with an average westward speed of only 1 cm sec^{-1}. It then turned south along the western boundary, accelerated to over 50 cm sec^{-1}, and continued south along the boundary all the

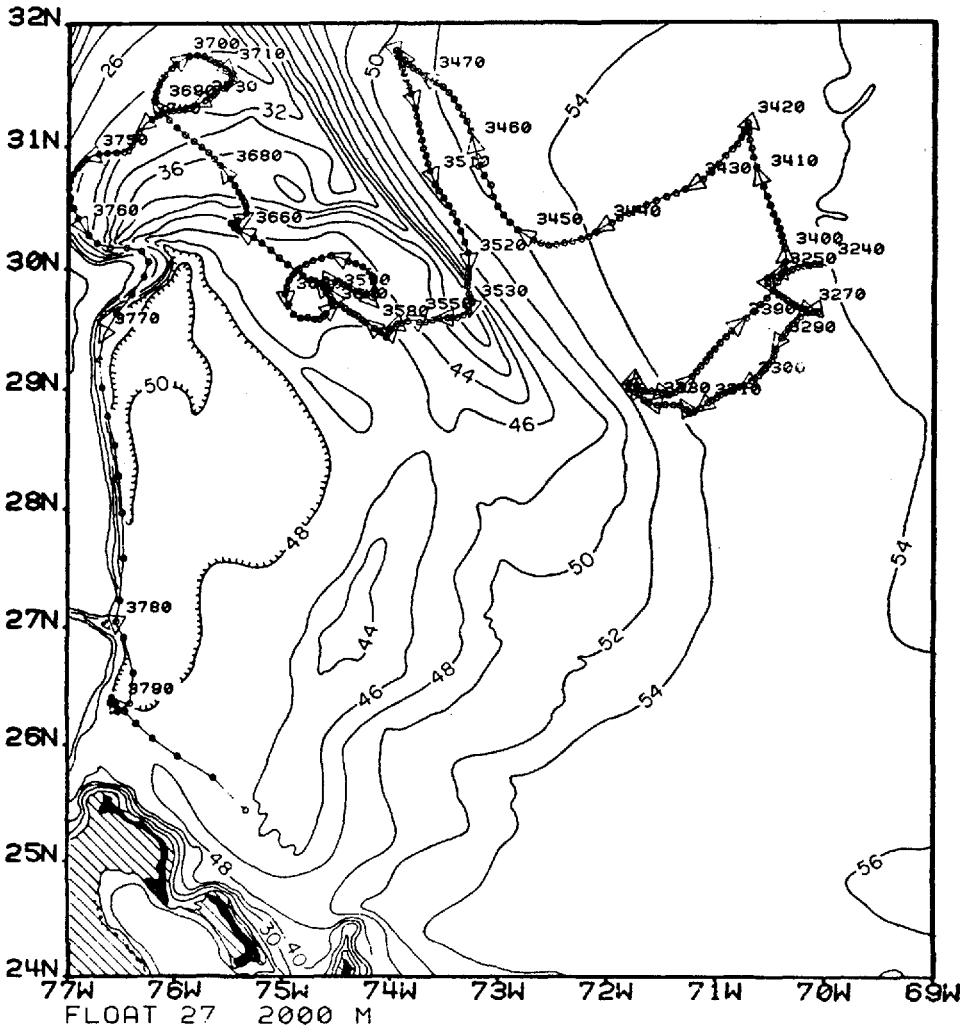

Figure 18. As for float 25, but for float 27, at 2000 m.

way to 24.5N, 75W, indicating an unusually strong current at a depth of 2000 m. This trajectory is very similar to three of the trajectories of MODE floats (at around 1800 m) which showed evidence of a swift, south flowing jet along the Blake Escarpment (Riser *et al.*, 1978). In this case and in each of those cases fluid was apparently entrained into a deep, western boundary current from the mid-ocean.

8. Discussion

At this point, it is useful to summarize the essential results of the observations reported. From SOFAR float trajectories we infer considerable geographical vari-

ability to the character and strength of the mesoscale circulation at both 700 m and 2000 m in the western North Atlantic. In the thermocline, in a region south of 31N and roughly including the greater MODE region, there is only a very weak (< 1 cm sec^{-1}) mean flow. The residence time of particles in this region appears to be sometimes on the order of at least one year based on the trajectories of floats 25 and 30, shown here in detail, and much of the other 700 m data in this region as well. The greater MODE region also appears to be an area where locally the kinetic energy in the thermocline is at a minimum. Little particle exchange appears to be taking place across 31N at the 700 m level in this region. In other regions of the western North Atlantic, however, a different picture emerges. To the north of the greater MODE region, there is a suggestion of recirculation not unlike that proposed by Worthington (1976). There is some evidence of the existence of this recirculation extending to about 60W. To the south and east of the greater MODE region, still another regime is present: particle motions are predominantly zonal, and most often to the east, with typical speeds high enough that over the course of two years particles could travel from the western boundary to the Mid-Atlantic Ridge, with little or no net meridional displacement over that time.

In the deeper waters of the western North Atlantic, at 2000 m, there is indication that particle motions are affected by bottom topography, though the bottom is generally 3000 m or more below the level of observation. Deep trajectories from west of 67W indicate that the Blake-Bahama Outer Ridge seems often to play an important role in determining the character of the deep circulation within a few hundred kilometers of the western boundary. Very near the western boundary of the basin, at the Blake Escarpment, an intense (> 50 cm sec^{-1}) south flowing jet has been observed on several occasions during MODE and POLYMODE, indicating that at least intermittently there are substantial southward transports at depth near the western boundary. This may be compared to the numerical results of Holland (1978), which indicated the presence of small, semipermanent eddy-induced gyres in the deep water near the western boundary, having locally large transports near the boundary. South of mid-latitudes, the transport in the deep water near the boundary in the model was most often to the south, perhaps in agreement with the observations.

At depth in the Nares Abyssal Plain region, perhaps the "ocean interior," particle motions are very slow, and even in a region of the deep ocean only 5° square the residence times of particles may be at least 3 years, perhaps much longer; relative particle dispersion in such regions may be very weak. In addition, there is indication from float trajectories of an energy containing scale considerably longer than that observed nearer the western boundary. Such observations give a flavor for how different the deep ocean interior may be from the abyssal waters in the more intensely studied western boundary regime.

The data suggest that the characteristic zonal time scales are longer than the

meridional in the upper ocean, and at depth over a flat bottom. This observation is not unanticipated: Rhines (1976) discusses the tendency to such anisotropy in process oriented numerical models, and he shows how, as a final state, such anisotropy may result from any of a number of possible initial turbulent states. Rhines (1973, 1975) shows how, in a beta-plane homogeneous ocean, there is a tendency for the energy in a field of geostrophic turbulence to cascade to both small frequency and small wavenumber. Ordinary Rossby waves, however, associate small frequency with large wavenumber—hence linear Rossby modes, at least as they are usually considered, alone cannot describe this final state. According to Rhines, the final state of the cascade should be a very low frequency (almost steady) band of zonal flow, alternating with a scale width of $L_\beta \sim (2\ U/\beta)^{1/2}$, where U is a typical barotropic velocity. If we take $U \sim 10$ cm sec^{-1}, $\beta \sim 2 \times 10^{-13}$ cm^{-1} sec^{-1}, then $L_\beta \sim 100$ km. From the observations reported here, however, it is difficult to look for changes over meridional distances such as this, as adequate spatial coverage is generally not available.

From historical hydrographic data there is indirect evidence that, south of roughly 26N in the western North Atlantic, an eastward Eulerian mean flow exists in the thermocline, and the measurements reported here might be interpreted to suggest a mean eastward Lagrangian flow as well. Reid (1978) has reviewed both the literature and historical data and has concluded that the subtropical western North Atlantic circulation consists of essentially two gyres; in the upper ocean, the northernmost of these is an anticyclonic gyre not unlike that of Worthington (1976); the southernmost is cyclonic and can be traced completely across the basin from the western boundary to the eastern boundary. The meridional boundary between these two gyres is at approximately 30N and is a trough of low pressure extending nearly across the basin. To the north of this latitude we have evidence of anticyclonic recirculation (the trajectory of float 26). To the south, our observations of eastward flow may be part of a cyclonic gyre. Thus, the trajectory data reported here seems not qualitatively inconsistent with Reid's proposed circulation.

It is perhaps useful to compare the North Atlantic circulation with the corresponding circulation in the subtropical North Pacific. There, a zonally banded structure (not unlike that suggested from theory by Rhines (1975)) obtains in the upper ocean which seems to be a permanent part of the general circulation (Hasunuma and Yoshida, 1978). One of the more prominent bands, near 25N, has been named the Subtropical Countercurrent and has been observed repeatedly over a number of years. The Subtropical Countercurrent is assumed (from hydrographic observations) to flow to the east in the upper ocean; moreover, its existence has been explained as a simple consequence of Sverdrup-type dynamics (Yoshida and Kidokoro, 1967). Thus the overall circulation may be a complex mix of directly wind-driven and eddy-induced flows.

Whether or not the float observations in the North Atlantic also indicate the

presence of a Subtropical Countercurrent remains an open question. New quasi-Lagrangian experiments presently underway should help to further elucidate the spatial and temporal structure of the flow in subtropical western North Atlantic and should help to resolve this problem.

Acknowledgments. This work formed one portion of the first author's doctoral dissertation at the University of Rhode Island. Many people contributed to this effort both at the University of Rhode Island and Woods Hole Oceanographic Institution. The floats were expertly designed and prepared in Woods Hole under the direction of Mr. Douglas Webb. Dr. Albert Bradley designed and built the autonomous listening stations which allowed us to explore in regions beyond the range of land-based receivers. Mr. Donald Dorson of the University of Rhode Island ably built and maintained the shore-based listening stations. Ms. Diane Spain and Mr. Christopher Polloni of URI directed the software and hardware operations used in tracking the floats, often a difficult task in this developmental phase. We thank these and all the other people who participated in this effort, both ashore and at sea.

This work was generously supported by the National Science Foundation, Office of the International Decade of Ocean Exploration under grants IDO 75-18930, OCE-7818662, OCE-79-26187, and OCE-78-18662-AO2 and by the Office of Naval Research under contract N00014-76-C-0226. The final manuscript was prepared while one of us (S.R.) was supported by the Joint Institute for the Study of the Atmosphere and Ocean at the University of Washington. This work is POLYMODE Contribution Number 158.

APPENDIX

Statistical estimation from the data

In computing mean velocities and kinetic energies from the float data, it is necessary to have an estimate of the number of independent observations, in order to have a measure of the expected errors in the computations. It is possible to rigorously derive such error estimates from first principles; here, we shall use the criteria given by Flierl and McWilliams (1977) (hereafter FM).

Number of degrees of freedom in the mean velocity estimates. Suppose the data in a box consists of N sample velocities which are a sum of a true mean part $\bar{u}_i$ and a fluctuating part u_i, where the subscript denotes the zonal or meridional direction for $i=1$ or 2. Further, assume that this total velocity field is normally distributed. Let ϵ_{mi} be the mean square error in estimating the mean $\bar{u}_i$ from the finite number of samples. FM have shown that

$$\epsilon_{mi} = \frac{2}{N} \int_0^\infty R_{ii}(\tau)\, d\tau = \frac{2<u_i^2> I_{ii}}{N}$$

where R_{ii} is the autocovariance of u_i and I_{ii} is the integral time scale defined in Section 3 above. This relation is thus identical to the well-known relation for the error in estimating the mean of a normally distributed random variable if we identify the number of independent samples ν_{mi} as

$$\nu_{mi} = \frac{N}{2I_{ii}} .$$

The standard deviation of the mean estimate is then $\epsilon^{\frac{1}{2}}_{mi}$. The errors given in Tables 3 and 4 for the mean values computed from the data are $2\epsilon^{\frac{1}{2}}_{mi}$, or approximate 95% confidence limits.

Note that, in practice, the number of independent samples is reduced by one whenever a

Table A1. Values of the Lagrangian integral and square integral time scale used in estimating the number of independent samples for different geographic regions.

Region	Depth (m)	Floats reference	I_{11} (days)	I_{22} (days)	J_{11} (days)	J_{22} (days)
Zonal	700	Figure 6	18	7	44	19
Nares	2000	Figures 9a, b	15	7	37	18
Greater MODE	700	Figures 17, 18	13	8	36	22
Greater MODE	2000	*	12	10	18	19

* Computed in Freeland *et al.* (1975) for floats at a nominal depth of 1500 m and used for floats in the greater MODE region at 2000 m here.

pair of floats is closer than one length scale of the energy containing eddies (taken to be 50 km in the western North Atlantic) in any box at a given time. However, this does not often occur due to the strategy used in deploying floats in these experiments.

The values of the integral time scale I_{ii} used in computing these standard errors were arrived at using the following procedure. At 700 m, estimates of I_{ii} for the greater MODE region (see Table A1) were used for Regions 1 and 2, while estimates from the Zonal floats (Fig. 6) were used for Region 3. At 2000 m, the greater MODE region estimates from 1500 m (FRR) were used in all boxes west of 67W (Region 1) while the Nares estimates were used east of this longitude (Region 2). The integral time scale estimates were chosen in this manner to reflect the general behavior of the floats in a given region. However, it is inevitable that there is some uncertainty in such a procedure. For example, the I_{ii} estimates for the greater MODE region at 700 m (Region 1) are also used for the area to the north (Region 2), where the recirculation regime is clearly present; there are, however, too few observations in this region to obtain meaingful estimates of I_{ii}. In addition, while the data used to compute the integral time scale for the Zonal floats extend from 73W to 49W, the values of I_{ii} computed from this data were used in estimating the number of independent samples only east of 67W. At 2000 m, the greater MODE region estimates are applied to data as far west as 77W, where clearly float tracks are of a different character than those a few degrees farther east (Fig. 18). Such situations, however, involve only a small portion of the data.

Number of degrees of freedom in the eddy kinetic energy estimates. FM have shown that the mean-square error $\epsilon_{\sigma i}$ in estimating the velocity variance is

$$\epsilon_{\sigma i} = \frac{2}{N} \int_0^\infty R_{ii}^2(\tau)\, d\tau = \frac{2\langle \bar{u}_i^2 \rangle^2 J_{ii}}{N}$$

where J_{ii} is the square integral time scale,

$$J_{ii} = \lim_{T_\tau \to \infty} \langle \bar{u}_i^2 \rangle^{-2} \int_0^{T_\tau} R_{ii}^2(\tau)\, d\tau .$$

By analogy with the previous computation for the mean, the number of independent samples for purposes of estimating the variance, $\nu_{\sigma i}$, is then

$$\nu_{\sigma i} = \frac{N}{2J_{ii}} .$$

The values of the J_{ii} for different regions are given in Table A1. The values of J_{ii} used regionally were chosen in a manner analogous to that used for the I_{ii} estimates previously discussed. The resulting values of $\nu_{\sigma i}$ are used in applying the F-test to the ratio of zonal to meridional eddy kinetic energies in Section 2.

Estimates of the mean temperature field. In computing the autocovariance function of temperature and temperature-displacement correlations, it is necessary to remove the mean temperature from the temperature measured along the trajectories. Since the floats can cover substantial distances over their lifetimes, it is necessary to have some estimate of the variation of the mean temperature along float paths. In the 700 m temperature autocovariances computed here, this mean has been estimated and removed as follows. First, the temperature field at 700 m for the western North Atlantic, averaged in 2° latitude by 3° longitude squares as given in Lai and Richardson (1977), was used as an initial estimate of the mean temperature field in the region 21-29N, 59-74W. Since these estimates were constructed from expendable bathythermograph (XBT) data, some correction to these results was necessary due to the known systematic error in XBT temperature discussed in McDowell (1977); stated simply, below about 300 m, at any given depth measured by the XBT, the XBT temperature is too cold. At 700 m, this temperature error is roughly .5°C; the exact form for the correction used here was $T = .9375\ T_{LR} + 1.1875$, where T is the corrected temperature and T_{LR} is the original Lai-Richardson estimate. After correcting the mean temperature values in each square, a function of the form

$$\hat{T} = ax^3 + by^2 + cx + dy + exy + f$$

was fit by least squares to the corrected Lai-Richardson mean values, where $\hat{T}$ is the estimated temperature and x and y are distances in kilometers east and north of some reference point, taken here as 24N, 72W. The fit was quite good: in all cases the values of $\hat{T}$ at the data points were within .2°C of the corrected Lai-Richardson values. This function was then subtracted from the 700 m float temperatures at each x and y along float paths. For the corrected temperatures, it was found that $a = 2.15 \times 10^{-7}$, $b = -1.09 \times 10^{-6}$, $c = -6.17 \times 10^{-4}$, d = 2.06×10^{-3}, $e = 2.04 \times 10^{-7}$, and $f = 11.90$.

At the 2000 m level, the mean temperature removed from float trajectories in the Nares Abyssal Plain region (the only 2000 m temperature autocovariance presented here) was simply the ensemble mean temperature measured along the trajectories (3.59°C), since historically there have been few stations taken to this depth in this region of ocean.

REFERENCES

Crease, J. 1962. Velocity measurements in the deep water of the western North Atlantic. J. Geophys. Res., *67*, 3173–3176.

Ebbesmeyer, C. C. and B. A. Taft. 1979. Variability of potential energy, dynamic height, and salinity in the main pycnocline of the western North Atlantic. J. Phys. Oceanog., *9*, 1073–1089.

Flierl, G. R. and J. C. McWilliams. 1977. On the sampling requirements for measuring moments of eddy variability. J. Mar. Res., *35*, 797–820.

Freeland, H. J., P. B. Rhines and H. T. Rossby. 1975. Statistical observations of the trajectories of neutrally buoyant floats in the North Atlantic. J. Mar. Res., *33*, 383–404.

Hasunuma, K. and K. Yoshida. 1978. Splitting of the Subtropical Gyre in the western North Pacific. J. Oceanog. Soc. Japan, *34*, 160–172.

Holland, W. R. 1978. The role of mesoscale eddies in the general circulation of the ocean — numerical experiments using a wind-driven quasi-geostrophic model. J. Phys. Oceanog., *8*, 363–392.

Jenkins, W. J. and P. B. Rhines. 1980. Tritium in the deep North Atlantic Ocean. Nature, *286*, 877-880.

Lai, D. Y. and P. L. Richardson. 1977. Distribution and movement of cyclonic Gulf Stream rings. University of Rhode Island, Graduate School of Oceanography, Technical Report 77-1, 140 pp.

McDowell S. E. 1977. A note on XBT accuracy. POLYMODE News No. 29. Woods Hole Oceanographic Institution, Unpublished manuscript.

McDowell, S. E. and H. T. Rossby. 1978. Mediterranean water: an intense mesoscale eddy off the Bahamas. Science, *202*, 1085–1087.

MODE-1 Group. 1978. The Mid-Ocean Dynamics Experiment. Deep-Sea Res., *25*, 859–910.

Pratt, R. M. 1968. Atlantic Continental Shelf and Slope of the United States — Physiography and Sediments of the Deep-Sea Basin, Geological Survey Professional Paper 529-B, U.S. Government Printing Office.

Reid, J. L., Jr. 1978. On the mid-depth circulation and salinity field in the North Atlantic Ocean. J. Geophys. Res., *83*, 5063–5067.

Rhines, P. B. 1973. Observations of the energy containing eddies, and theoretical models of waves and turbulence. Boundary Layer Meteorology, *4*, 345–362.

—— 1975. Waves and turbulence on a beta-plane. J. Fluid Mech., *69*, 417–431.

—— 1976. The dynamics of unsteady currents, *in* The Sea, 6, E. D. Goldberg *et al.*, eds., John Wiley, New York.

Richman, J. G., C. Wunsch and N. G. Hogg. 1977. Space and time scales of mesoscale motion in the western North Atlantic. Rev. Geophys. Space Phys., *16*, 385–420.

Riser, S. C. 1982a. The quasi-Lagrangian nature of SOFAR floats. Deep-Sea Res., (in press).

—— 1982b. Quasi-Lagrangian dynamical signatures of mesoscale circulation in the mid-ocean, (in preparation).

Riser, S. C., H. J. Freeland and H. T. Rossby. 1978. Mesoscale motions near the deep western boundary of the North Atlantic. Deep-Sea Res., *25*, 1179–1191.

Rossby, H. T. 1982. Eddies and the general ocean circulation. Proceedings of the Conference on the Present and Future of Oceanography. Woods Hole Oceanographic Institution.

Rossby, H. T., A. D. Voorhis and D. Webb. 1975. A quasi-Lagrangian study of mid-ocean variability using long range SOFAR floats. J. Mar. Res., *33*, 355–382.

Schmitz, W. J. 1978. Observations of the vertical distribution of low frequency kinetic energy in the western North Atlantic. J. Mar. Res., *36*, 295–310.

Snedecor, G. W. and W. G. Cochran. 1967. Statistical Methods, 6th Edition. Iowa State University Press, 593 pp.

Stommel, H. M. 1958. The abyssal circulation. Deep-Sea Res., *5*, 80–82.

Stommel, H. M., P. Niiler and D. Anati. 1978. Dynamic topography and recirculation of the North Atlantic. J. Mar. Res., *38*, 449–468.

Sverdrup, H. U., M. W. Johnson and R. H. Fleming. 1942. The Oceans. Their Physics, Chemistry, and General Biology. Prentice-Hall, 1087 pp.

Taylor, G. I. 1921. Diffusion by continuous movements. Proc. London Math. Soc. A, *20*, 196–211.

U.S. Department of Commerce. 1978. Gulfstream, *4*, U.S. Government Printing Office.

von der Haar, T. H. and A. H. Oort 1973. New estimates of the annual poleward energy transport by northern hemisphere oceans. J. Phys. Oceanog., *3*, 169–172.

Webb, D. 1977. SOFAR floats for POLYMODE. Conference Record, Oceans '77, Volume 2. IEEE-Marine Technology Society.

Worthington, L. V. 1976. On the North Atlantic circulation. Johns Hopkins University Oceanographic Studies, *6*, 110 pp.

Wunsch, C. 1978. The North Atlantic general circulation west of 50W determined by inverse methods. Rev. Geophys. Space Phys., *16*, 583–620.

Yoshida, K. and T. Kidokoro. 1967. A subtropical countercurrent (II)—a prediction of eastward flows at lower subtropical latitudes. J. Oceanogr. Soc. Japan, *23*, 231–246.

Received: *22 December, 1980*; revised: *28 September, 1982.*